*34th EPS Conference on Plasma Phys. Warsaw, 2 - 6 July 2007 ECA Vol.**31F**, P-2.060 (2007)*

Pressure profile shape constancy in L-mode stellarator plasmas

A.V. Melnikov[1], L.G. Eliseev[1], I. Pastor[2], J. Herranz[2], C. Hidalgo[2], A. Fujisawa[3], T. Minami[3], K.A. Razumova[1], Yu.N. Dnestrovskij[1], S.E. Lysenko[1] and J.H. Harris[4]

[1] *Nuclear Fusion Institute, RRC "Kurchatov Institute", Moscow, Russia,*

[2] *Laboratorio Nacional de Fusión, EURATOM-CIEMAT, Madrid, Spain*

[3] *National Institute for Fusion Science, Toki, Japan*

[4] *Fusion Energy Division, Oak Ridge National Laboratory, USA*

It is well known that the temperature profiles in a tokamak are self-consistent [1-3]. For the stellarators there is no temperature profile consistency [4]. The pressure profile consistency concept works in tokamaks [5]. There was found one example of the pressure profile stiffness in the pellet injection versus gas puff experiments in LHD [6]. The paper is dedicated to the investigation of this concept for the stellarators. Plasma temperature and density profile evolution during NBI heating of on- and off- axis ECRH heated plasma on TJ-II [7], for ECRH power scan on W7-AS [8] and CHS [9], high T_i mode on CHS [10], on- and off- axis ECRH on W7-AS [4] and gas puffing on ATF [11] were observed (see Table 1).

In the TJ-II stellarator, NBI heating (P_NBI = 300 kW) of the target ECRH plasma (P_ECRH = 300 kW) leads to dramatic changes of the plasma density and temperature. n_e and T_e profile evolution measured by high resolution Thomson Scattering diagnostics is shown in Fig.1 [7]. The values varied up to an order of magnitude, ($0.3 < n_e(0) < 6\times10^{19}$ m^{-3}, $0.2 < T_e(0) < 1$ keV), the profiles varied from hollow to peaked (density), and from peaked to flat (electron temperature). In spite of the large difference in n_e and T_e profiles in the analyzed regime, their product, the plasma pressure P_e, presents much stronger profile resilience in the confinement zone of the plasma column. It was found that the normalized pressure profiles $P^{norm} = P(\rho)/P(0)$ are much less scattered in comparison with plasma n_e and T_e profiles, see Fig. 2.

In the CHS experiments with on-axis P_{EC} = 150÷215 kW and density $n_e = (0.47÷0.95)\times10^{19}$ m^{-3} variation [9], the similar behavior was found: the increase of T_e was accompanied by the decrease of n_e, leaving $P^{norm}(\rho)$ practically unchanged. In the experiments with the standard major plasma axis (R_ax=92.1cm, $n_e(0)= 4\times10^{19}$ m^{-3}, $T_e(0)$~$T_i(0)$=250 eV), and optimized one (R_ax=87.7cm, $n_e(0)= 2\times10^{19}$ m^{-3}, $T_e(0)$=200 eV, $T_i(0)$=130 eV) [10], the same tendency was found, P^{norm} remains almost constant. In high T_i mode ($n_e(0)= 1.4\times10^{19}$ m^{-3}, $T_e(0)$=700 eV, $T_i(0)$=1 keV) [10], P^{norm} almost coincides with the rest of discussed CHS profiles.

In W7-AS experiment with on-axis P_{EC} variation from 0.2 to 0.8 MW at almost the same density n_e~2×10^{19} m^{-3} [8], the similar behavior was found: increase of T_e was accompanied by a decrease of n_e, remaining P^{norm} (ρ) practically unchanged. In another experiment, on- and off- axis ECRH alternate with corresponding T_e and n_e variations [4]. It is highlighted in [4] that during off-axis ECRH (ρ=0.6) the central density is peaking without an additional particle source. It leaded to almost unchanged P^{norm} (ρ).

At the gas puffing in the ATF [11], the plasma density rise was accompanied by the concordant decay of T_e, again remaining P^{norm} (ρ) practically unchanged.

Despite the difference in the magnetic configurations (heliac TJ-II, heliotron CHS, torsatron ATF, optimized W7-AS), a remarkable similarity is seen in the normalized pressure profiles, in other words, the normalized pressure profile has universal shape for normal confinement (L-mode) in all the observed experiments (see Fig. 2). The universal profiles can be fitted by a quasi-linear function in the confinement zone (0.2 < ρ < 0.8), $P_0^{-1}dP/d\rho$ ~ const = k = $P_0^{-1}\Delta P_{linear}/\Delta\rho_{linear}$, $\Delta\rho_{linear}$ is the radial extension, where profile has almost linear shape. In the observed cases $\Delta\rho_{linear}$~0.6, $k\approx1.3 \pm 0.1$ (in Table 1, Δk is thelinear regression error for k).

Table 1.

Device	Type	R, m	a, m	B, T	$\iota/2\pi(a)$	$-k$	Δk	Regime, [Ref.]
TJ-II	heliac	1.5	0.22	1.0	1.6, low shear	1.34 1.39	0.04 0.04	EC-on +NBI [7] EC-off +NBI [7]
W7-AS	modular coils	2.0	0.2 0.16 0.13	2.5	low shear, 0.56	1.19 1.28 1.38	0.02 0.02 0.02	P_{EC} scan, n_e-const [8] EC on-off [4] HDH vs NC [12]
CHS	helio-tron	0.92	0.19	0.9 1.9 1.9 1.9	strong shear	1.32 1.39 1.36 1.29	0.02 0.02 0.02 0.02	EC-on, n_e-var [9] EC-on, ITB [10] High T_i, NBI 1MW R_{ax}-var., n_e-var. [10]
ATF	torsatron	2.1	0.27	1.9	shear	1.11	0.02	Gas puff [11]

Contrary to the L-mode, pressure profiles show different shapes during improved confinement modes. An example of the edge transport barrier is shown in Fig. 2b. P^{norm}(ρ) in HDH confinement mode in W7-AS [12] differs strongly from universal profile, while the reference Normal Confinement profile belongs to the universal one. Strong similarity of the profiles allows us to get any spatial point in the confinement area for the normalization, not only ρ=0. In case of ITB formation the pressure profiles have clearly two components. The outer component (outside the ITB), normalized at the ITB foot, shows the pressure profiles similarity (the universal profile takes place), while inside the ITB area $P_{ITBfoot}^{-1}dP/d\rho$ is significantly higher. Fig. 3 shows W7-AS data with on-axis P_{EC} =1.2 MW, where the temperature and pressure profiles show the ITB formation at ρ ~ 0.25 [8]. In CHS ITB was obtained for on-axis ECRH (B=1.9T, P_{EC} = 0.3 MW at 106GHz) at ρ ~ 0.4 [10]. In both cases

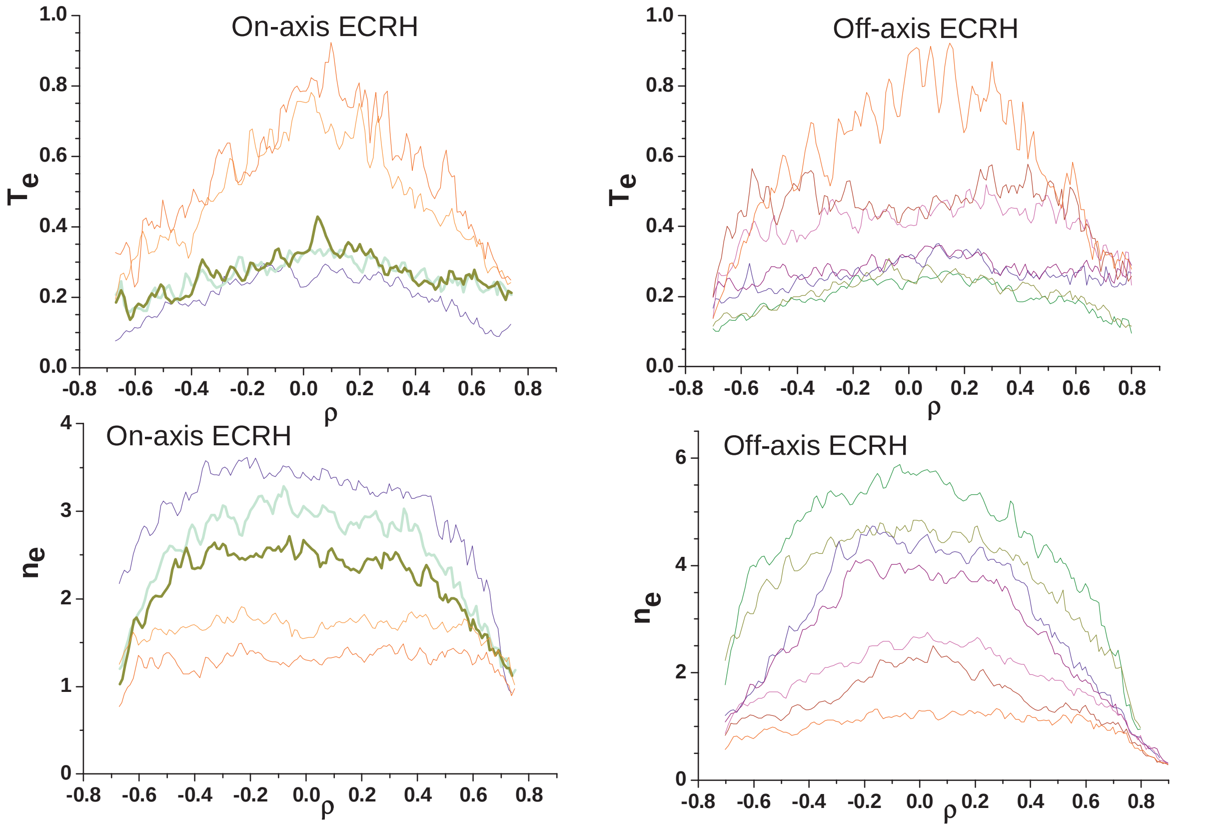

Fig 1. T_e (upper) and n_e (lower) profile evolution in the NBI experiments for on axis (left) and off-axis (right) ECRH in TJ-II. Time passes from red to blue curves.

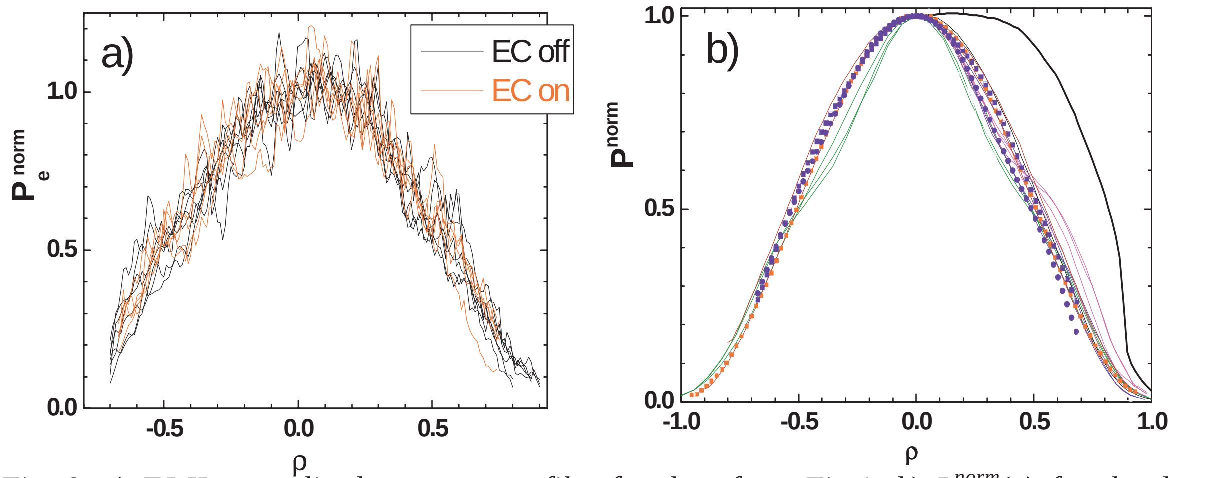

Fig. 2. a) TJ-II normalized pressure profiles for data from Fig.1; b) $P^{norm}(\rho)$ for the data presented in table forms the universal profile; CHS: red dots – high T_i mode, brown – R_{ax} variaton, red – P_{EC} variation; ATF: purple - gas puff; W7-AS: green - P_{EC}-on scan, blue - EC-on- and off-axis, black – HDH-mode, dark blue – reference Normal Confinement mode; TJ-II: blue dots – EC on-, off-axis. Profiles from all machines and experiments were radially normalized to the actual plasma size, $P^{norm}(1)=0$.

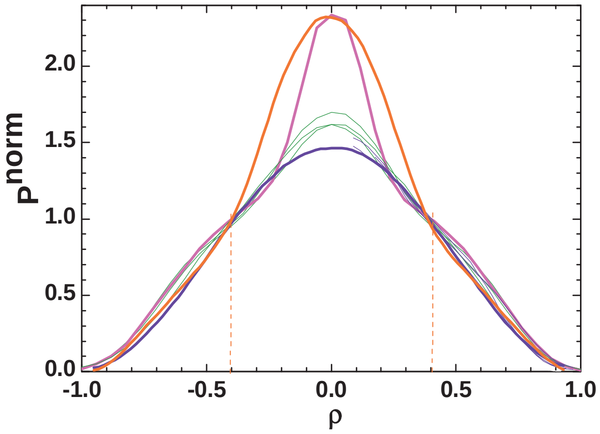

Fig. 3. The universal profile features outside the ITB area. CHS: blue – high T_i mode, red – ITB; W7-AS: green – P_{EC} =0.2-0.8 MW, pink – ITB (P_{EC}=1.2 MW); P^{norm}=P/P ($\rho_{ITBfoot}$= 0.4)

outside the ITB area, the profiles coincide with the universal one.

Summary. (I) In spite of large variety in the profiles of plasma electron temperature and density, their product, electron pressure presents the feature of profile constancy in stellarator devises in observed experiments with wide range of the plasma and heating parameters.

(II) In the L-mode plasmas of the medium size stellarators, the pressure profiles show remarkable similarities between each other in low (TJ-II, W7-AS) and high (CHS, ATF) magnetic shear configurations. So, the universal profile, characterized by $P_0^{-1}dP/d\rho$ ~ const = k, was found for L-mode plasmas and outside the ITB area. The other types of profile like in case of LHD [6] may take place for specific plasma conditions. (III) The observation of the universal constant k in L-mode (e.g. in the absence of strong E×B effects) may suggests that turbulence and the associated transport reach some kind of saturation level, that does not depend on the absolute values of T_e and n_e, but alternative explanations (e.g. based on the role of atomic physics and links between magnetic configuration and gradient) can not be excluded The validation of the transport-based hypothesis would require to characterize the link between local gradients and turbulent transport.

Kurchatov team was supported by Goscontract 02.516.11.6068 and Grants RFBR 05-02-17016, 07-02-01001, INTAS 100008-8046, NWO-RFBR 047.016.015.

References

[1] B. Coppi, Comments Plasma Phys. Control. Fusion 5 261 (1980)
[2] Yu.V. Esiptchuk and K.A. Razumova, Plasma Phys. Control. Fusion 28 1253 (1986)
[3] F. Ryter et al., Plasma Phys. Control. Fusion 43 A323 (2001)
[4] F. Wagner et al., Phys. Plasmas 12, 072509 (2005)
[5] Yu.N. Dnestrovskij et al., Nucl. Fusion 46 953 (2006)
[6] H. Yamada et al., Nucl. Fusion 41, 7 901 (2001)
[7] M. Liniers et al., 15 ISW, Madrid, 2005, P3-14
[8] V. Erckmann et al., In: “Radio Frequency Power in Plasmas”, AIP (1999)
[9] H. Nakano. Private communication
[10] S. Okamura et al., Nucl. Fusion 39, 9Y, 1337 (1999)
[11] M. Shats et al., Phys. Plasmas 2 (2) 398 (1995)
[12] K. McCormick, Phys. Rev. Lett, 89, 015001 (2002)